THE JOURNAL OF BIOLOGICAL CHEMISTRY VOL. 281, NO. 33, pp. 23377–23385, August 18, 2006

The N-terminal Ricin Propeptide Influences the Fate of Ricin A-chain in Tobacco Protoplasts*

Received for publication, March 22, 2006, and in revised form, June 13, 2006 Published, JBC Papers in Press, June 14, 2006, DOI 10.1074/jbc.M602678200

Nicholas A. Jolliffe[‡1], Alessandra Di Cola[‡1], Catherine J. Marsden[‡], J. Michael Lord[‡], Aldo Ceriotti[§], Lorenzo Frigerio[‡], and Lynne M. Roberts[‡2]

From the [‡]Department of Biological Sciences, University of Warwick, Coventry CV4 7AL, United Kingdom and the [§]Istituto di Biologia e Biotecnologia Agraria, Consiglio Nazionale delle Ricerche, Via Bassini 15, 20133 Milano, Italy

The plant toxin ricin is synthesized in castor bean seeds as an endoplasmic reticulum (ER)-targeted precursor. Removal of the signal peptide generates proricin in which the mature A- and B-chains are joined by an intervening propeptide and a 9-residue propeptide persists at the N terminus. The two propeptides are ultimately removed in protein storage vacuoles, where ricin accumulates. Here we have demonstrated that the N-terminal propeptide of proricin acts as a nonspecific spacer to ensure efficient ER import and glycosylation. Indeed, when absent from the N terminus of ricin A-chain, the non-imported material remained tethered to the cytosolic face of the ER membrane, presumably by the signal peptide. This species appeared toxic to ribosomes. The propeptide does not, however, influence catalytic activity *per se* or the vacuolar targeting of proricin or the rate of retrotranslocation/degradation of A-chain in the cytosol. The likely implications of these findings to the survival of the toxin-producing tissue are discussed.

Ricin is a heterodimeric protein produced in the seeds of the castor oil plant *Ricinus communis* where it accumulates in the protein storage vacuoles (PSV)[3] of endosperm cells. Mature ricin consists of a ribosome-inactivating A-chain (RTA) linked by a disulfide bond and non-covalent interactions to a galactose binding B-chain (RTB). This heterodimer is toxic to mammalian cells because it can bind via RTB to a variety of galactosylated cell surface molecules and, following retrograde transport to the endoplasmic reticulum (ER) and delivery of RTA to the cytosol, irreversibly inactivate ribosomes. RTA is a potent *N*-glycosidase that depurinates 28 S/25 S/26 S ribosomal RNA (1, 2) at a site in the ribosome that is critical for binding elongation factor-2 ternary complexes (3, 4). This leads to a halt in protein synthesis and, ultimately, cell death.

Although the ribosomes of *Ricinus* endosperm cells are susceptible to RTA-mediated depurination (5), intoxication of the producing tissue is avoided. Co-translational ER import is accompanied by *N*-glycosylation (6), disulfide bond formation (7), and proteolytic cleavage of the signal peptide (8), the first 26 residues of a 35-residue presequence at the N terminus of preproricin (9) (Fig. 1). Imported proricin consists of a 9-residue N-terminal propeptide, the mature RTA sequence, a 12-residue linker propeptide, and RTB. This precursor is catalytically inactive (10) because the RTB moiety sterically obstructs the substrate binding site of RTA, as it does in mature ricin heterodimers. In this form, proricin is delivered to PSV, and the mature RTA-RTB heterodimer is generated by the endoproteolytic removal of both the N-terminal and internal propeptides (7, 11–14). Ricin holotoxin accumulates within the confines of the endosperm vacuoles to 5% of the total particulate protein (15, 16).

The ricin precursor and its constituent subunits have been well studied in the heterologous system of tobacco protoplasts (17–20). Although it is clear that the 26-residue signal peptide mediates ER import and that the 12-residue linker propeptide is essential for vacuolar targeting (21), the role of the 9-residue N-terminal propeptide remains to be determined. Here we address this by examining the fate of precursors to ricin and ricin A-chain expressed with or without this propeptide, again in tobacco protoplasts. Our data show that the 9-residue propeptide influences both co-translational import and the extent of RTA glycosylation and also suggest that it may contribute to prevention of damage to endogenous ribosomes.

EXPERIMENTAL PROCEDURES

Recombinant DNA—All DNA constructs were generated in the expression vector pDHA (22). Expression constructs encoding ppRT, pRTA, pRTB, and phaseolin (pDHE-T343F) have been described previously (19, 23). The ricin active site substitution E177D has also been previously documented (24). All derivative constructs used in this work were generated by the QuikChange™ method (Stratagene) using the following mutagenic primers (and their reverse complements, not shown): The N-terminal propeptide was deleted using 5′-GGATCCACCTCAGGGATATTCCCCAAACAATACC-3′; the signal peptide was deleted using 5′-CCTCTAGAGTCGAGGATGTGGTCTTTCACATTAGAGG-3′; the signal peptide and N-terminal propeptide were deleted together using 5′-CCTCTAGAGTCGAGGATGATATTCCCCAAACAATACCC-3′; the first and second glycosylation sites were disrupted using 5′-CCAAACAATACCCAATTATACAATTTACCACAGCGGGTGCC-3′ or 5′-CCAATTCAACTGCAAAGACGTCAA-

* This work was supported by Biotechnology and Biological Sciences Research Council Grant C17404 (to L. F. and L. M. R.) and a WT program grant (to L. M. R. and J. M. L.). The costs of publication of this article were defrayed in part by the payment of page charges. This article must therefore be hereby marked "*advertisement*" in accordance with 18 U.S.C. Section 1734 solely to indicate this fact.

[1] Both authors contributed equally to this work.

[2] To whom correspondence should be addressed. Tel.: 44-2476-523558; Fax: 44-2476-523701; E-mail: lynne.roberts@warwick.ac.uk.

[3] The abbreviations used are: PSV, protein storage vacuoles; RIP, ribosome-inactivating protein; RTA, ricin A-chain; RTB, ricin B-chain; ER, endoplasmic reticulum.

GGTTCCAAATTCAGTGTG-3′, respectively; the Gly-10 to Val substitution was introduced into pRTA or ΔRTA using 5′-GGATCCACCTCAGTGTGGTCTTTTCACATTAG-3′ or 5′-GGATCCACCTCAGTGATATTCCCCAAACAATACC-3′, respectively; the Gly-10 to Val, Ser-8 to Val double substitution was introduced into pRTA using 5′-GGATCCAC-CTCAGTGTGGGTTTTCACATTAGAGG-3′; the last 8 residues of the propeptide were substituted for Gly in pRTA using 5′-GGATCCACCTCAGGGTGGGGAGGAGGAGG-AGGAGGAGGAGGAATATTCCCCAAAC-3′; the Lys-4 to Gly substitution was made in pRTA using 5′-CCTCA-GGGATATTCCCCGGACAATACCCAATTATAAAC-3′.

Transformation of Protoplasts and Pulse-Chase Experiments—Protoplasts were prepared from axenic leaves (4–7 cm long) of *Nicotiana tabacum* cv. Petit Havana SR1. Protoplasts were subjected to polyethylene glycol-mediated transfection, radiolabeled with Pro-Mix (Amersham Biosciences), and chased as described previously (19). In some experiments, before radioactive labeling, protoplasts were incubated for 1 h at 25 °C in K3 medium supplemented with 50 μg/ml tunicamycin (5 mg/ml stock in 10 mM NaOH; Sigma). At the desired time points, 3 volumes of cold W5 medium were added and protoplasts were pelleted by centrifugation at 60 × *g* for 10 min at 4 °C. Cells were frozen on dry ice and stored at −80 °C.

Protoplast Fractionation—Protoplast pellets (from 500,000 cells) were resuspended in 170 μl of sucrose buffer (100 mM Tris-HCl, pH 7.6, 10 mM KCl, 1 mM EDTA, 12% (w/w) sucrose, supplemented with Complete protease inhibitor mixture (Roche Applied Science)) and homogenized by pipetting 50 times with a Gilson-type micropipette though a 200-μl tip. Intact cells and debris were removed by centrifugation for 5 min at 500 × *g*. From the 160 μl recovered, 32 μl was saved and directly used for immunoprecipitation. The remainder was loaded on a 17% (w/w) sucrose pad and centrifuged at 100,000 × *g* for 30 min at 4 °C. Pellets (microsomes) and supernatants (soluble proteins) were diluted in protoplast homogenization buffer and used for immunoprecipitation.

Protease Protection Assay—Protoplast pellets (from 500,000 cells) were homogenized in 12% sucrose buffer as described above, but omitting protease inhibitors, and debris was removed by spinning at 500 × *g* for 5 min. Supernatants were divided into three aliquots and incubated for 30 min at 25 °C with either buffer (as a control) or proteinase K (5 mg/ml stock in 50 mM Tris-Cl, pH 8, 1 mM $CaCl_2$; Calbiochem) at a final concentration of 75 μg/ml in the presence or absence of 1% Triton X-100. Phenylmethylsulfonyl fluoride was added to 20 mM final concentration to inhibit proteinase K before immunoprecipitation.

Preparation of Protein Extracts and Immunoprecipitation—Frozen samples were homogenized by adding protoplast homogenization buffer (19) supplemented with Complete protease inhibitor mixture (Roche Applied Science). Homogenates were used for immunoprecipitation with polyclonal rabbit anti-RTA, anti-BiP (23), or anti-phaseolin antisera. Immunoselected polypeptides were analyzed by 15% SDS/PAGE. Gels were treated with Amplify (Amersham Biosciences) and radioactive polypeptides revealed by fluorography. Densitometry was performed using Aida image analyzer (v.3.11).

Toxicity Measurements—Triplicate aliquots of 330,000 protoplasts were co-transfected with a toxin-encoding plasmid or empty vector (pDHA) and the phaseolin-encoding construct pDHET343F. After 16 h of recovery, protoplasts were pulse labeled for 1 h before being pelleted as described. Polypeptides immunoselected from homogenates using anti-phaseolin antiserum were separated on SDS-PAGE before fluorography and densitometry as before. Toxicity of the various constructs was expressed as percentage of phaseolin synthesis with respect to protoplasts co-transfected with empty vector instead.

Expression and Purification of pRTA and ΔRTA—Ricin A-chain including the 9-residue propeptide from native ricin (pRTA) was generated by PCR mutagenesis and standard recombinant DNA techniques using the RTA expression plasmid pUTA (25) as a PCR template. Both ΔRTA and pRTA were expressed using the same protocol. A single colony of *Escherichia coli* JM101 transformed with the pUTA vector containing either the pRTA or ΔRTA sequence was used to inoculate 50 ml of 2YT and grown overnight at 37 °C. This starter culture was used to inoculate 500 ml of 2YT, and the culture was grown for 2 h at 30 °C. Expression was induced by adding isopropyl 1-thio-β-D-galactoside to a final concentration of 0.1 mM for 4 h at 30 °C. Cells were harvested by centrifugation at 2740 × *g*, resuspended in 15 ml of 5 mM sodium phosphate buffer, pH 6.5, and lysed by sonication on ice. Cell debris was pelleted by centrifugation at 31,400 × *g* at 4 °C for 30 min and the supernatant loaded onto a 50-ml CM-Sepharose CL-6B column (Amersham Biosciences). The column was washed with 1 liter of 5 mM sodium phosphate, pH 6.5, followed by 100 ml of 100 mM NaCl in 5 mM sodium phosphate, pH 6.5; RTA was eluted with a linear gradient of 100–300 mM NaCl in the same buffer. Fractions containing pRTA or ΔRTA were pooled and stored at 4 °C at a concentration of no more than 1 mg/ml.

N-Glycosidase Activity Assay of pRTA and ΔRTA—The activity of both pRTA and ΔRTA was determined by assessing their ability to depurinate 26 S rRNA of purified yeast (*Saccharomyces cerevisiae*) ribosomes. For each reaction, 20 μg of yeast ribosomes were incubated at 30 °C with 10 nM ΔRTA or pRTA for increasing times in 25 mM Tris-Cl, pH 7.6, 25 mM KCl, 5 mM $MgCl_2$, in a total volume of 20 μl. Reactions were stopped by the addition of 100 μl of 2× Kirby buffer (6 g of 4-amino salicylic acid (Na^+ salt) in 100 mM Tris, pH 7.6, 20 mM KCl, 2% tri-isopropyl-naphthalene sulfonic acid) and 80 μl of H_2O. rRNA was obtained by precipitation after two phenol-chloroform extractions. 4 μg of rRNA were treated with 20 μl of acetic-aniline for 2 min at 60 °C to hydrolyze the now labile phosphoester bond at the depurinated site. rRNA was precipitated and resuspended in 15 μl of 60% de-ionized formamide/0.1× TPE (3.6 mM Tris, 3 mM NaH_2PO_4, 0.2 mM EDTA) and heated at 65 °C for 5 min. Ribosomal RNA fragments were separated on a 1.2% agarose, 0.1× TPE, 50% formamide gel. rRNAs were quantified from digital images of ethidium bromide-stained gels using ImageQuant software, and depurination in each lane was calculated by relating the amount of any rRNA fragment released upon aniline treatment with the amount of 5.8 S rRNA (directly proportional to the quantity of 26 S rRNA) and expressing values as percentages after correcting intensities according to rRNA size.

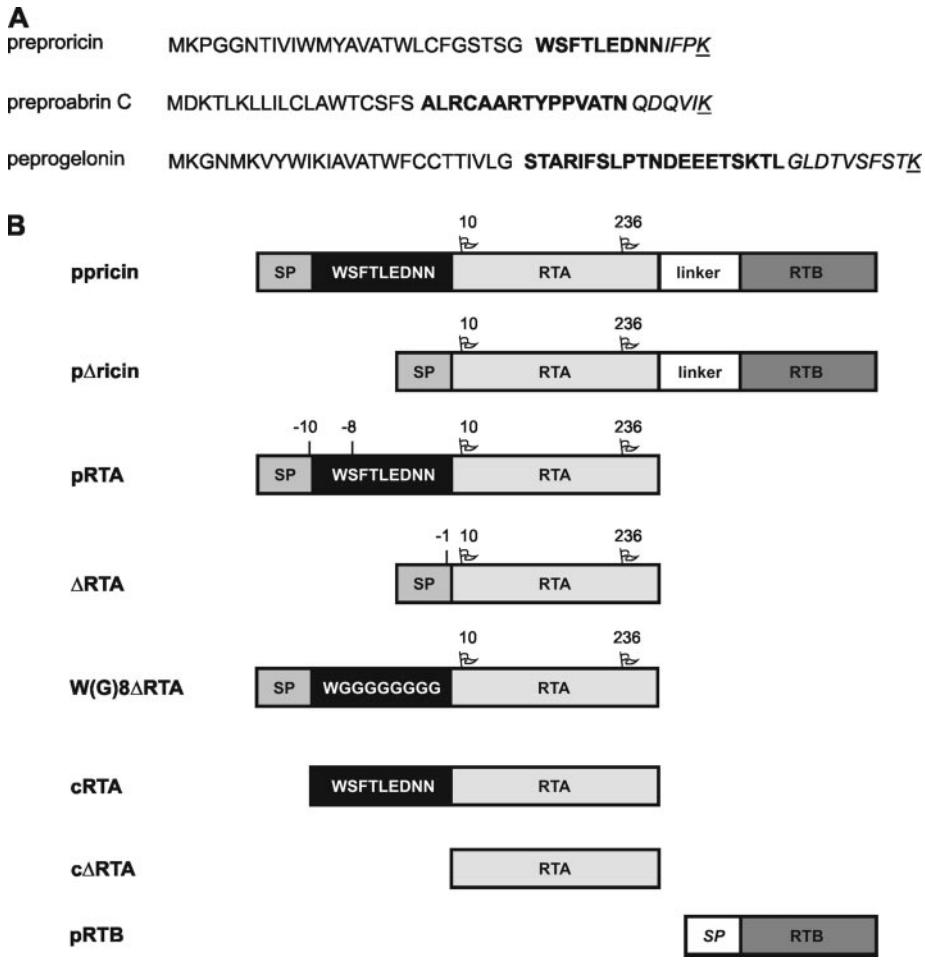

FIGURE 1. *A*, comparison of presequences from three ribosome-inactivating proteins. ER signal peptides are followed by putative propeptides (*bold*), which in turn are followed by the mature RIP domains (*italics*). *B*, sequences expressed in tobacco protoplasts. All ricin-related cDNA sequences were cloned into vector pDHA and their expression driven by a CaMV35S promoter fused to an untranslated alfalfa mosaic virus leader. *ppricin*, full-length preproricin; *SP*, 26-residue signal peptide of preproricin; *SP*, β-phaseolin signal peptide. The *black box* denotes constructs containing the N-terminal 9-residue propeptide (not drawn to scale). The position of potential glycosylation sites (*flags*, *N10* and *N236*) and of mutations introduced into the signal peptide/propeptide region are indicated.

RESULTS

The Ricin Propeptide Affects the Efficiency of Glycosylation—In the few cases where the sequence of the mature N terminus of ribosome-inactivating proteins is known, it is possible to compare the cDNA presequences (Fig. 1*A*). The signal peptide cleavage site can be predicted with high accuracy using the SignalP 3.0 server (26). In the case of preproricin (9), preproabrin C (27), and preprogelonin (28), non-conserved amino acid segments are present between the signal peptidase cleavage site and the mature domain (Fig. 1*A*). To analyze the function of the 9-residue N-terminal propeptide of preproricin *in vivo* we generated a mutant preproricin lacking this sequence (Fig. 1, pΔricin) and compared its fate in tobacco mesophyll protoplasts with that of wild type. Because RTA has been shown to be active on tobacco ribosomes (29), these and all other ricin-based constructs described herein were generated in the background of an active site mutation (E177D) (24) unless otherwise stated. Transfected protoplasts were pulse labeled for 1 h with [^{35}S]methionine and [^{35}S]cysteine and then chased for 5 h. Immunoprecipitation with anti-RTA antiserum revealed pΔricin expression comparable with that of wild type (Fig. 2*A*, compare *lanes 3* and *5*). After 5 h of chase, no immunoreactive species were recovered from the medium, with both wild-type and mutant precursor polypeptides (*gray arrowheads*) instead being processed to yield mature RTA and RTB (Fig. 2*A*, *lanes 4* and *6*, *open arrowheads*). We have previously demonstrated that this processing occurs in vacuoles (7). The N-terminal propeptide does not, therefore, affect the targeting of the ricin precursor to this compartment.

An additional, faster migrating band was generated from pΔricin upon chase (Fig. 2*A*, *lane 6*, *black arrowhead*). To determine the origin of this band we generated a version of the RTA subunit lacking the N-terminal propeptide (ΔRTA) and co-expressed this with RTB in tobacco protoplasts. Again, a faster migrating band was immunoprecipitated from cells expressing ΔRTA, but not pRTA (Fig. 2*B*, *lane 5*, *black arrowhead*), confirming that it was A-chain derived. ΔRTA, like pRTA, was able to assemble with RTB, and the heterodimer was subsequently secreted into the medium (Fig. 2*B*). This is expected, as it lacks the vacuolar sorting signal, the 12-residue propeptide normally linking RTA and RTB in the ricin precursor. To characterize the faster migrating protein further, we expressed pRTA or ΔRTA in the presence of the glycosylation inhibitor tunicamycin or its solvent alone (Fig. 3*A*). As expected for a glycosylated protein, pRTA synthesized in the presence of tunicamycin migrated more quickly than that synthesized in its absence (Fig. 3*A*, compare *lanes 3* and *4*). Likewise, the largest form of ΔRTA is not detected in the presence of tunicamycin (Fig. 3*A*, compare *lanes 5* and *6*). Comparison with pRTA (*lanes 3* and *4*) suggests that the smallest form of ΔRTA (*lane 5*, *black arrowhead*) is non-glycosylated. Furthermore, the difference in mobility between non-glycosylated pRTA (*lane 4*) and non-glycosylated ΔRTA (*lowest band*, *lane 6*) is compatible with lack of the 9-residue propeptide. To confirm that the extra, faster migrating band observed on gels following ΔRTA expression was indeed a non-glycosylated ΔRTA, we generated mutants of pRTA and ΔRTA lacking one or both *N*-glycosylation sites. Asn residues at positions 10 and 236 (Fig. 1) were therefore replaced with Gln. For both pRTA and ΔRTA, the phenotype of the N10Q mutation was indistinguishable from that observed upon tunicamycin treatment (compare Fig. 3*A*, *lanes 3–6*, and Fig. 3*B*, *lanes 2*, *3*, *6*,

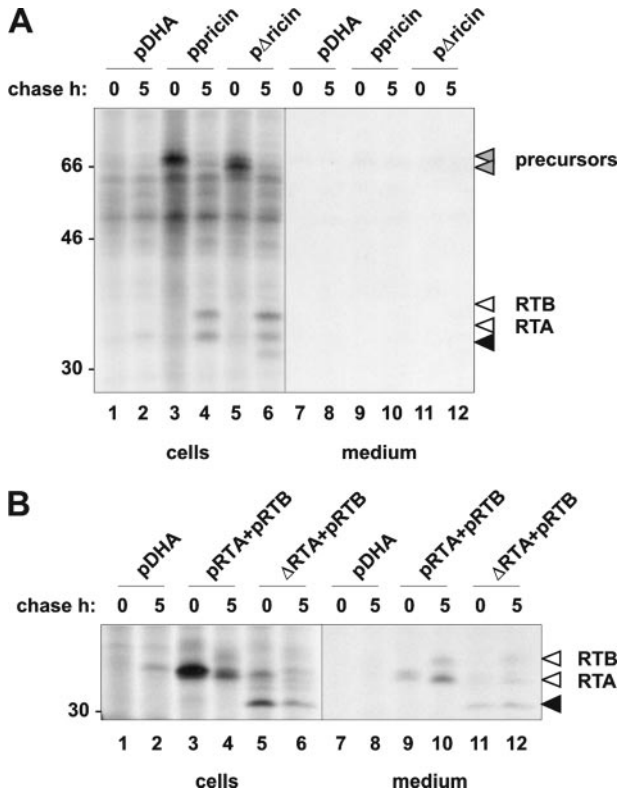

FIGURE 2. **Synthesis and fate of preproricin or RTA/RTB heterodimers lacking the N-terminal propeptide.** *A*, protoplasts were transfected with empty vector alone (*pDHA*) or constructs encoding preproricin (*ppricin*) or preproricin lacking the N-terminal propeptide (*pΔricin*). Protoplasts were labeled with [^{35}S]cysteine and [^{35}S]methionine for 1 h and chased for 5 h. RTA was immunoprecipitated from cell homogenates and incubation medium with anti-RTA antiserum and analyzed by reducing SDS/PAGE. *B*, protoplasts were transfected with empty vector alone (*pDHA*) or co-transfected with vectors encoding ER-targeted ricin B-chain (*pRTB*) and either ricin A-chain (*pRTA*) or ricin A-chain lacking the N-terminal propeptide (*ΔRTA*) and analyzed as in *panel A*.

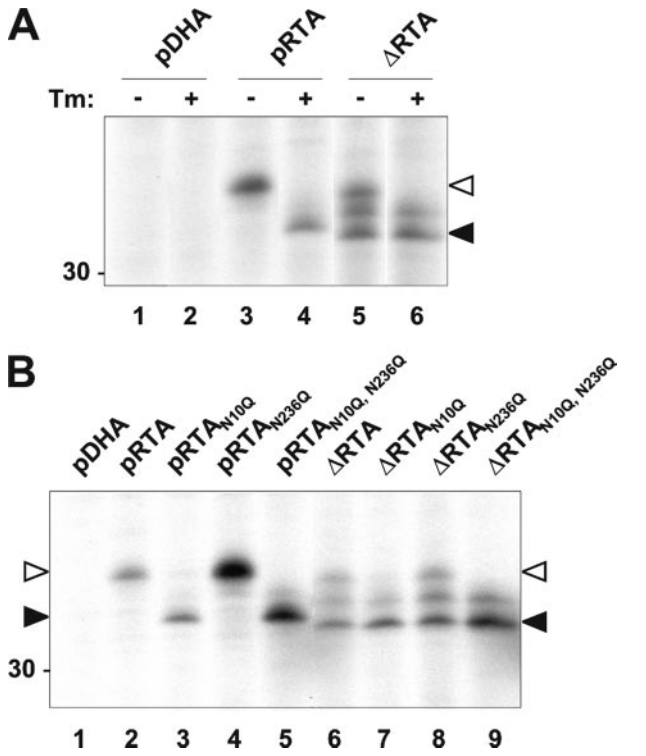

FIGURE 3. **Glycosylation of free ricin A-chain when expressed with or without the N-terminal propeptide.** *A*, protoplasts were transfected with empty vector (*pDHA*) or constructs encoding pRTA or ΔRTA. Protoplasts were preincubated for 1 h in the presence of either 10 mM NaOH (−) or 50 μg/ml tunicamycin (*Tm*) in 10 mM NaOH (+) and then radiolabeled with [^{35}S]cysteine and [^{35}S]methionine for 1 h. RTA was immunoselected from cell homogenates with anti-RTA antiserum and analyzed by reducing SDS/PAGE. *B*, protoplasts were transfected with empty vector (*pDHA*), or constructs encoding pRTA or ΔRTA, and pRTA or ΔRTA in which one (*N10 or N236*) or both (*N10 and N236*) glycosylation sites were mutated. Protoplasts were radiolabeled with [^{35}S]cysteine and [^{35}S]methionine for 1 h and analyzed as in *panel A*.

and *7*). In contrast, expression of the N236Q mutants did not affect the mobility of either protein (Fig. 3*B*, *lanes 2* and *4* and *lanes 6* and *8*), showing that only the N-terminal of the two potential *N*-glycosylation sequons ever receives a glycan when RTA is expressed in tobacco protoplasts. These data show that by deleting the N-terminal propeptide, the efficiency of glycosylation at the first sequon (Asn-10) in both the ricin precursor and isolated A-chain is reduced.

The Ricin Propeptide Influences ER Import—When ΔRTA polypeptides were immunoselected and resolved by SDS-PAGE a third protein, with a mobility between the glycosylated and non-glycosylated ΔRTA, was also reproducibly detected (Fig. 3, *A* and *B*). To probe the identity of this species, we first investigated its intracellular fate. Protoplasts expressing either pRTA or ΔRTA were homogenized and total microsomal membranes prepared by centrifugation through a 17% sucrose pad. Clearly, this form of ΔRTA (*open arrowhead*) remained associated with membranes throughout the time course (Fig. 4*A*, *M*, *lanes 14*, *17*, *20*, and *23*). By contrast, the glycosylated and non-glycosylated forms of ΔRTA (*black arrowheads*) behaved like pRTA in that, following sequestration within the ER (microsomes (*M*) in Fig. 4*A*) during synthesis, they were subsequently retrotranslocated to the cytosol (soluble fractions (*S*) in Fig. 4*A*) in the chase. The size of the stably membrane-associated ΔRTA was consistent with it being non-glycosylated and bearing an uncleaved signal peptide. To test this, we resolved pRTA and ΔRTA immunoprecipitates from tobacco protoplasts alongside the same proteins translated *in vitro* in the absence of microsomal membranes (Fig. 4*B*). The intermediate-sized ΔRTA form that was generated in tobacco cells co-migrated with the equivalent *in vitro* translated product (Fig. 4*B*, compare *lanes 4* and *5*, *open arrowhead*). This strongly suggests that this was indeed signal peptide-uncleaved, non-glycosylated A-chain. Signal peptide cleavage after residue 26 of preproricin is clearly predicted in both pRTA and ΔRTA by the SignalP 3.0 server (26). We therefore reasoned that the persistence of the signal peptide was more likely due to a defect in co-translational import, preventing exposure of the sequence to signal peptidase. As the standard fractionation analysis (Fig. 4*A*) does not allow us to distinguish between lumenal ΔRTA and any ΔRTA bound to the surface of the microsomes, this was clarified using a protease protection assay (Fig. 4*C*). Unlike the lumenal chaperone BiP (Fig. 4*C*, *lower panel*) and glycosylated or non-glycosylated signal peptide-cleaved RTA (*upper panel*, *black arrowheads*), the putative signal peptide-uncleaved ΔRTA (*open arrowhead*) was fully sensitive to protease attack in the absence of detergent (compare *lanes 13* and *14* and *16* and *17*). This is consistent

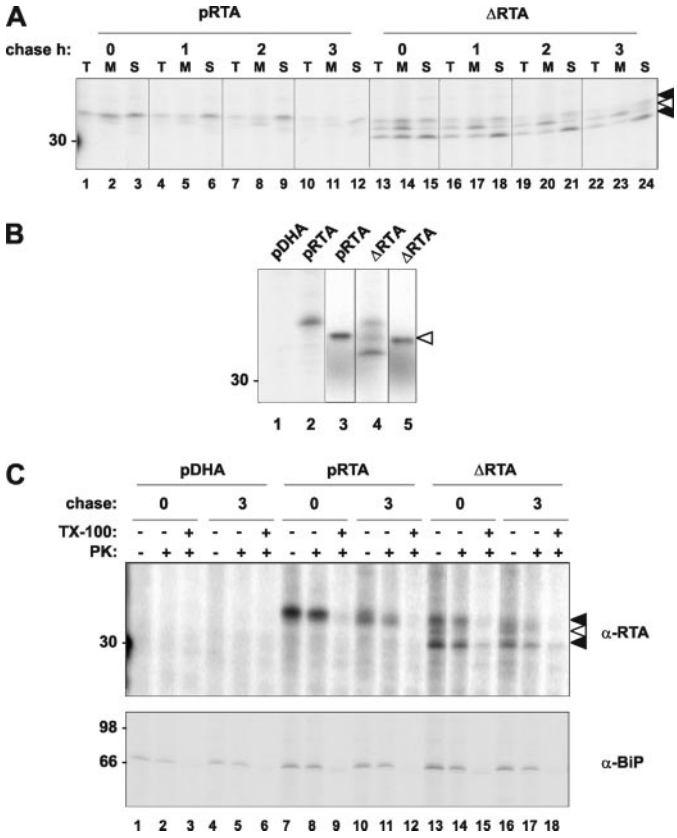

FIGURE 4. **Subcellular localization of signal peptide uncleaved RTA.** *A*, protoplasts were transfected with constructs encoding pRTA or ΔRTA. Protoplasts were labeled with [^{35}S]cysteine and [^{35}S]methionine for 1 h and chased for 1, 2, and 3 h before being homogenized in the absence of detergent. An aliquot of the homogenate was saved (*T*) and the remainder centrifuged to yield microsomal (*M*) and soluble (*S*) fractions. Proteins were immunoselected with anti-RTA antiserum and analyzed by SDS-PAGE and fluorography. *B*, protoplasts were transfected either with empty vector (*pDHA*) or as in *panel A* before labeling with [^{35}S]cysteine and [^{35}S]methionine for 1 h. RTA was immunoselected from cell homogenates with anti-RTA antiserum. Immunoselected proteins were resolved by SDS/PAGE (*lanes 1*, *2*, and *4*) along with *in vitro* translations of the same RTA-encoding sequences (*lanes 3* and *5*) performed in the absence of microsomal membranes. *C*, protoplasts were transfected as in *panel B* and homogenized as in *panel A* before dividing three ways and incubating in the absence or presence of proteinase K (*PK*) and detergent (*TX-100*) as indicated. Proteins were immunoselected sequentially using anti-RTA and anti-BiP antisera and resolved as in *panel A*.

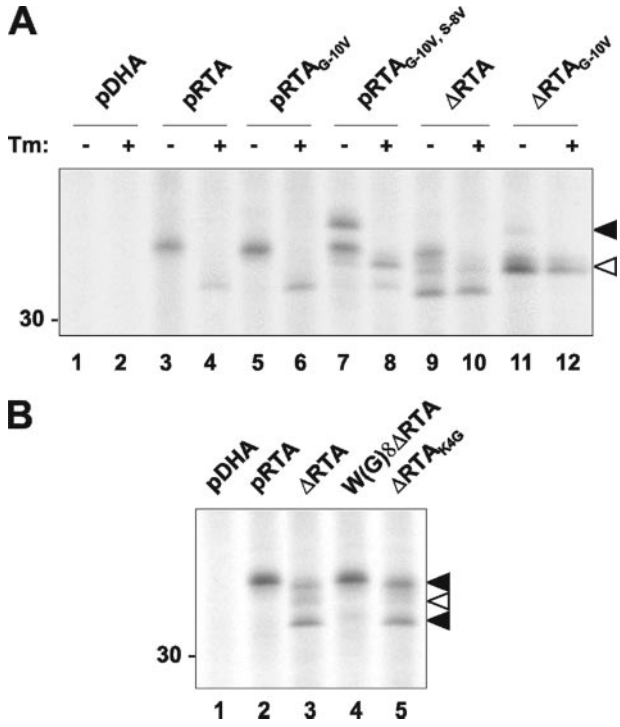

FIGURE 5. *A*, protoplasts were transfected with empty vector (*pDHA*) or constructs encoding pRTA or ΔRTA or these constructs mutated at predicted sites of signal peptide cleavage. Protoplasts were preincubated for 1 h in the presence of either 10 mM NaOH (−) or 50 μg/ml tunicamycin (*Tm*) in 10 mM NaOH (+) and then labeled with [^{35}S]cysteine and [^{35}S]methionine for 1 h. RTA was immunoselected from cell homogenates with anti-RTA antiserum and analyzed by reducing SDS/PAGE. *B*, protoplasts were transfected with empty vector (*pDHA*) or constructs encoding pRTA, ΔRTA, W(G)8ΔRTA, or ΔRTA$_{K4G}$ radiolabeled and analyzed as in *panel A*.

with the cytosolic exposure of a non-imported, membrane-tethered species of RTA.

Although lack of ER import explains why the signal peptide-uncleaved ΔRTA is not glycosylated, a proportion of the correctly imported and processed ΔRTA also failed to receive a glycan. One reason for this may be that the glycosylation site at Asn-10 of the mature domain of RTA is too close to the membrane during import, prior to signal peptide cleavage, for efficient glycosylation by oligosaccharyl transferase. To investigate this, we generated mutants of pRTA and ΔRTA with the intention of preventing signal peptide cleavage and analyzed whether these proteins became glycosylated by comparing them with equivalent forms produced in tunicamycin-treated cells. Mutation of the predicted signal peptide cleavage site in pRTA, by replacement of Gly with Val at position −10, was ineffective in preventing signal peptide removal (Fig. 5*A*, *lanes 5* and *6*). Alternative cleavage occurred, most probably at the nearby Ser residue −8 within the propeptide (Signal P 3.0) (26). We therefore mutagenized both Gly-10 and Ser-8. Expression of the double mutant pRTA$_{G-10V,\ S-8V}$ yielded two RTA forms in roughly equal proportions. The larger protein displayed the gel mobility expected for a processed and glycosylated RTA carrying an uncleaved signal peptide (Fig. 5*A*, compare *lanes 3* and *7*). Correspondingly, this was absent when synthesized in the presence of tunicamycin (Fig. 5*A*, *lane 8*). Even though there is still some cleavage (Fig. 5*A*, *lane 7*, *lower band*), it is clear from this analysis that RTA containing the N-terminal propeptide can be glycosylated even when the signal peptide remains attached. By contrast, the signal peptide-uncleavable mutant ΔRTA$_{G-10V}$ (this mutation alone was sufficient to abolish cleavage in the absence of the propeptide) was almost completely non-glycosylated (Fig. 5*A*, *lane 11*). If the propeptide was acting as a spacer in this regard, we reasoned that the glycosylation of ΔRTA could be increased by inserting an artificial sequence in its place. We therefore generated W(G)$_8$ΔRTA (Fig. 1), in which the 9-residue propeptide was replaced by a Trp (to preserve the signal peptide cleavage site) and 8 Gly residues. Clearly, this product became glycosylated as efficiently as wild-type pRTA (Fig. 5*B*, compare *lanes 2* and *4*).

Interestingly, and in contrast to ΔRTA, there was no evidence of a signal peptide-uncleaved form of W(G)$_8$ΔRTA (Fig. 5*B*, compare *lanes 3* and *4*, *open arrowhead*), suggesting that the insertion of this spacer also served to improve co-translational import. Because charge distribution in the signal peptide and its flanking region can influence import (30), we substituted the

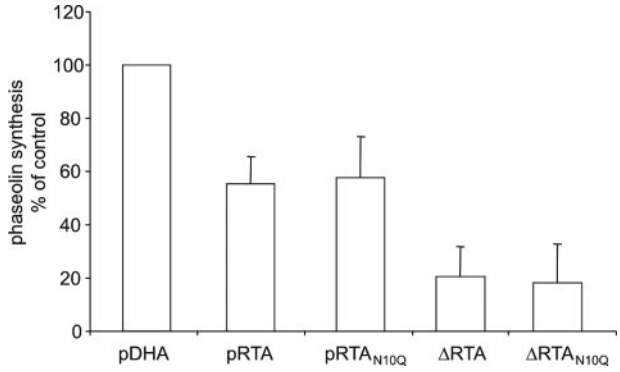

FIGURE 6. **Toxicity of ricin A-chains to tobacco ribosomes.** Triplicate preparations of protoplasts were co-transfected with empty vector (*pDHA*), or one of the indicated RTA-encoding constructs, and the phaseolin reporter construct. Protoplasts were labeled with [^{35}S]cysteine and [^{35}S]methionine for 1 h. The protein synthesis reporter, phaseolin, was immunoselected with anti-phaseolin antiserum and analyzed by reducing SDS/PAGE. The synthesis of β-phaseolin was measured by densitometry and expressed as the percentage of the control (*pDHA*). *Bars* indicate standard deviation.

first positively charged residue of mature RTA, Lys 4, with Gly (ΔRTA_{K4G}, Fig. 1). This substitution did indeed appear to improve ER import, with more ΔRTA_{K4G} instead appearing as the signal peptide cleaved, glycosylated form (Fig. 5*B*, compare *lanes 3* and *5*, *open arrowhead* and *upper black arrowhead*).

The Absence of the Propeptide Increases Toxicity of RTA—We have shown that deletion of the propeptide impaired ER import and resulted in inefficient glycosylation of RTA. However, the fraction of ΔRTA that is released into the ER lumen, either glycosylated or non-glycosylated, can still retrotranslocate into the cytosol (Fig. 4*A*, *lanes 15*, *18*, *21*, and *24*). We have previously shown that similarly dislocated pRTA is toxic to tobacco ribosomes. To test whether ΔRTA is also toxic, tobacco protoplasts were transfected with plasmids encoding pRTA, $pRTA_{N10Q}$, ΔRTA, or ΔRTA_{N10Q}, this time with functional active sites. As a protein synthesis reporter to monitor ribosome inactivation, cells were co-transfected with a plasmid encoding the bean storage protein phaseolin. We then immunoprecipitated phaseolin and compared its expression levels in the presence or absence of the various toxin mutants. Strikingly, ΔRTA was found to be 3-fold more toxic than pRTA (Fig. 6). This increase in toxicity was not due to the difference in glycosylation of ΔRTA, because the non-glycosylated mutant (ΔRTA_{N10Q}) was also three times more toxic than $pRTA_{N10Q}$ (Fig. 6).

If ΔRTA is more stable in the cytosol than its wild-type counterpart, then this could explain the difference in toxicity observed. To test this, we transfected protoplasts with constructs expressing non-glycosylated mutants of pRTA or ΔRTA and monitored their stability by pulse-chase analysis. Surprisingly, the rates of degradation of $pRTA_{N10Q}$ and ΔRTA_{N10Q} were very similar during this time course (Fig. 7*A*). It was also clear that the relative rates of dislocation from the ER, as assessed by monitoring disappearance from the membrane fraction with time, were similar for pRTA and ΔRTA (Fig. 4*A*). This indicated that the increased toxicity of ΔRTA was linked neither to a different rate of retrotranslocation nor to a higher stability of the protein in the cytosol.

Interestingly, and by striking contrast, RTA or ΔRTA expressed without their signal peptides (Fig. 1, *cRTA* and *cΔRTA*) were found to be relatively stable throughout the 3 h of chase (Fig. 7*A*). In light of the above, an obvious possibility for the increased potency of ΔRTA was that it possessed an enhanced catalytic activity. We used these stable cytosolic forms to investigate this, again by co-expressing with the reporter phaseolin, whose synthesis was then quantified (Fig. 7*B*). Clearly, however, the cytosolic forms of RTA and ΔRTA showed comparable toxicity. We also investigated potencies *in vitro* by expressing pRTA and ΔRTA in *E. coli*, purifying the proteins and measuring the *N*-glycosidase activity of these toxins against purified yeast ribosomes. In concurrence with our data *in vivo*, pRTA and ΔRTA were able to depurinate ribosomes with almost identical efficiency (Fig. 7*C*). According to these data, the greater toxicity of ΔRTA with respect to pRTA cannot be attributed to an increased catalytic activity either.

DISCUSSION

Ricin is synthesized in developing *R. communis* endosperm as a precursor (Fig. 1, *preproricin*) containing both the RTA and RTB moieties. In its unprocessed form, this precursor also contains a 26-residue signal peptide (9), followed by a 9-residue N-terminal extension preceding the RTA sequence, and a 12-residue internal sequence containing vacuolar sorting information linking RTA and RTB. Upon deposition in PSVs, the two propeptides are removed to generate mature, heterodimeric ricin (Fig. 8) (7, 11–14). In developing endosperm, ricin remains isolated in PSV until the seed germinates, when it becomes proteolytically degraded to provide a source of amino acids to fuel early post-germinative growth (31, 32). The vacuolar isolation of ricin in endosperm cells is essential, because *Ricinus* ribosomes are themselves susceptible to the RTA-mediated modification that accounts for the exquisite toxicity of ricin (5). The same principle applies to any potent ribosome-inactivating protein (RIP) that enters the secretory pathway.

Unlike other ricin-coding regions, the role of the 9-residue N-terminal propeptide is unknown. In the present study we have addressed the significance of this sequence using transient expression in tobacco protoplasts, a system whose efficacy in faithfully reproducing the biosynthesis of ricin has previously been demonstrated (17–20). Deleting the 9-residue propeptide from preproricin (pΔricin) appeared to have no significant effect on the synthesis of the precursor (Fig. 2*A*, compare *lanes 3* and *5*) or on its intracellular trafficking or processing in the vacuole (Fig. 2*A*, compare *lanes 4* and *6*). However, alongside glycosylated ΔRTA, a faster migrating polypeptide was observed whenever proricin or RTA forms lacking the N-terminal propeptide were expressed (Fig. 2, *A* and *B*, *black arrowhead*). Treatment with tunicamycin revealed that this species was non-glycosylated (Fig. 3*A*), a result confirmed by site-directed mutagenesis (Fig. 3*B*). Our analysis also demonstrated that when wild-type RTA was expressed in tobacco cells it became fully glycosylated, but only at a single site (Asn-10).

It is possible that the deletion of the propeptide may affect RTA glycosylation at this site in several ways. First, RTA glycosylation is almost fully dependent on signal peptide cleavage in the absence of the propeptide. Indeed, when signal peptide

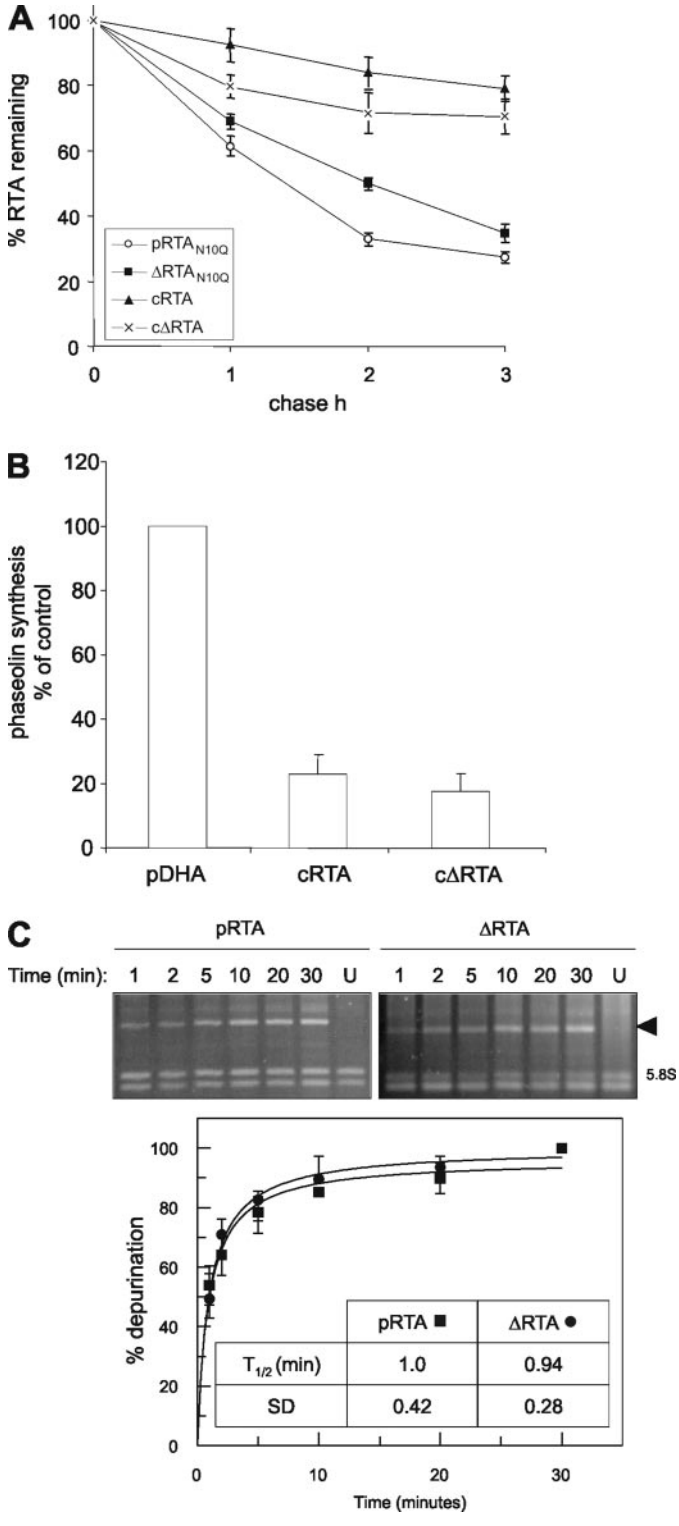

FIGURE 7. **Assessment of the rRNA *N*-glycosidase activity of pRTA and ΔRTA.** *A*, protoplasts were transfected with empty vector (pDHA) or constructs encoding non-glycosylated or cytosolic A-chains, with or without the propeptide, and labeled with [^{35}S]cysteine and [^{35}S]methionine for 1 h, and chased for the indicated times. RTAs were immunoselected from cell homogenates with anti-RTA antiserum and analyzed by reducing SDS/PAGE. The intensity of the immunoselected bands was measured by densitometry and expressed as a percentage of total RTA immunoselected after the pulse. The *graph* shows the average values from three independent experiments. *Bars* indicate standard deviation. *B*, triplicate preparations of protoplasts were co-transfected with empty vector (*pDHA*) or one of the indicated cytosolic RTA-encoding constructs, and the phaseolin construct. Protoplasts were labeled with [^{35}S]cysteine and [^{35}S]methionine for 1 h. Phaseolin was then immunoselected with anti-phaseolin antiserum and resolved by reducing SDS/PAGE. The synthesis of β-phaseolin was measured by densitometry and expressed as the percentage of the control (*pDHA*). *Bars* indicate standard deviation. *C*, 20 μg of isolated yeast ribosomes were incubated with 10 nM pRTA or ΔRTA for increasing times at 30 °C. Total rRNA was isolated, and 4-μg samples were treated with acetic-aniline, pH 4.0, and electrophoresed on a denaturing agarose/formamide gel. *U*, rRNA isolated from yeast ribosomes treated with pRTA or ΔRTA but not treated with aniline. The rRNA fragment released by aniline treatment of RTA-depurinated 26 S rRNA (*black arrowhead*) was quantified, along with the corresponding 5.8 S rRNA, from digital images using ImageQuant software, and percentage depurination was calculated. Symbols indicate the mean of experimental data ($n = 3$); *error bars* represent the standard deviation; *solid lines* represent best-fitted curves.

cleavage was artificially compromised by mutagenesis, glycosylation at Asn-10 was also almost entirely blocked in the fraction of ΔRTA that was imported. This is consistent with the observation that, in a model membrane protein, acceptor sites positioned too close to the luminal face end of a transmembrane segment could not be utilized *in vitro* (33). Second, the efficiency of RTA glycosylation is markedly reduced in the absence of the propeptide. The way in which the propeptide affects the interaction between the nascent chain and oligosaccharyl transferase is probably complex. Clearly, because signal peptide cleavage is a prerequisite for ΔRTA glycosylation, the time window during which RTA glycosylation can occur may be shorter in the absence of the propeptide. The propeptide could also affect the timing of signal peptide cleavage and/or the conformation of the N terminus of the mature protein, where Asn-10 is located, and thus modulate the accessibility of the glycosylation site in this way too (34). It is significant that when the last 8 residues of the propeptide were replaced with Gly, glycosylation was restored (Fig. 5*B*). This suggests that the propeptide is required to provide a physical separation between the signal peptidase cleavage site and Asn-10, rather than serving a sequence-specific function.

Expression and gel resolution of ΔRTA also revealed another immunoprecipitable band with a gel mobility lying between the glycosylated and non-glycosylated RTAs. This non-glycosylated A-chain remained membrane associated, whereas the other RTA forms were retrotranslocated to the cytosol with time. Further analysis identified this protein as being non-imported (Fig. 4*C*). Because this form of native RTA was never observed, we conclude that the N-terminal propeptide must somehow facilitate co-translational import or prevent the abortion of import. Recently, it has been proposed that cleavable signal peptides of secretory proteins invert during synthesis (35). This exposes the cleavage site to signal peptidase on the lumenal surface of the ER, leaves the N terminus pointing toward the cytosol, and allows the C terminus of the nascent chain to translocate into the lumen. Inversion is dependent on a number of factors, including the distribution of charged residues flanking the hydrophobic core and the length of the hydrophobic core itself (30). It is possible that the propeptide facilitates such signal peptide inversion in RTA. That the insertion of a string of Gly residues can compensate for the missing propeptide, permitting complete ER import, indicates that a region(s) immediately following the propeptide may be inhibitory to this inversion. The first charged residue in mature RTA (Lys-4) is a conserved and functionally important surface-exposed residue.

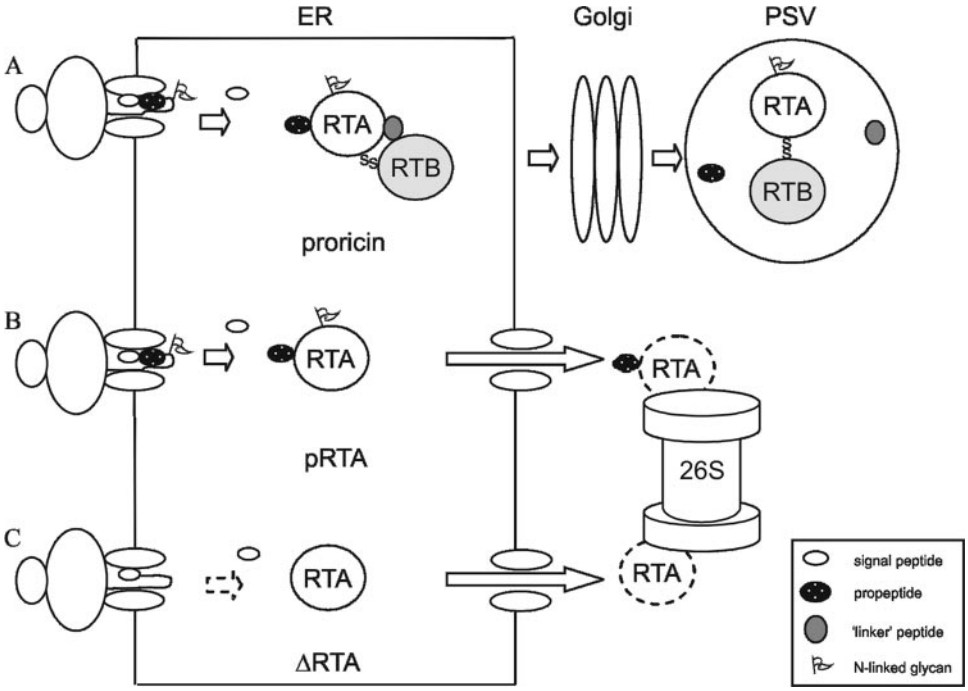

FIGURE 8. **Comparison of the intracellular fates of proricin, pRTA, and ΔRTA.** *A,* preproricin is synthesized as a single polypeptide precursor on ER-bound ribosomes. After cotranslational removal of the signal peptide, *N*-glycosylation, and disulfide bond formation, proricin travels through the Golgi complex and is sorted to the protein storage vacuole (*PSV*) by virtue of the vacuolar sorting signal contained in the 12-amino acid "linker" peptide that joins the A- and B-chains. In the PSV, both the N-terminal propeptide and the linker peptide are proteolytically cleaved to release mature heterodimeric ricin (19). *B,* pRTA is efficiently translocated into the ER lumen where signal peptide removal and *N*-glycosylation occur. pRTA is then retrotranslocated to the cytosol where it becomes deglycosylated, with most then being degraded by the 26 S proteasome (20). *C,* ΔRTA is also cotranslationally imported into the ER lumen. However, in this case both import and *N*-glycosylation are very inefficient (denoted by the *dashed arrow*), and a proportion of the protein remains associated with the membrane in a signal peptide-uncleaved form (not depicted). The proportion of ΔRTA that is released into the ER lumen is also retrotranslocated to the cytosol, being eventually degraded by the proteasome.

When this residue was replaced with Gly in ΔRTA, import was improved (Fig. 5*B*). This raises the possibility that the propeptide may serve to distance the Lys residue from the signal peptide, allowing it to be preserved at this N-proximal site.

In addition to the influence on ricin biosynthesis described above, we have also shown that the presence of the N-terminal propeptide significantly reduced the toxicity of RTA when expressed in tobacco protoplasts. Earlier work characterizing pRTA expression in tobacco has shown that ER-localized pRTA is able to undergo retrotranslocation to the cytosol, a process that results in the proteasomal degradation of most of the toxin (20, 36). However, a fraction of retrotranslocated toxin somehow uncouples from these steps to inactivate ribosomes and shut down protein synthesis. Intriguingly, although the presence of the propeptide markedly decreased the toxicity of ER-targeted RTA, neither its retrotranslocation into, nor its stability within, the cytosol appeared affected. The same was true when the difference in their glycosylation was eliminated. Most importantly, the catalytic activities of cRTA and cΔRTA, either directly expressed in the cytosol or produced recombinantly and exposed to purified ribosomes *in vitro*, were identical within the limits of our assays.

As described, another difference in behavior of pRTA and ΔRTA was the apparent partial failure to import the nascent chain of the latter. The resulting signal peptide-uncleaved ΔRTA is membrane tethered, presumably via the hydrophobic signal peptide, and is cytosolically exposed. It is possible that such an anchored RTA could correctly fold and therefore still possess enzymatic activity. Although the substrate rRNA in membrane-bound ribosomes would be too distant from the RTA active site, it is not improbable that cytosolic ribosomes, or indeed free 60 S subunits, could interact with the immobilized toxin. We therefore speculate that the functional ribosome population may be depleted as a result of progressive rRNA depurination in the free pool by membrane associated, stable ΔRTA. With the fraction of soluble, retrotranslocated ΔRTA acting apparently identically to pRTA, we believe that this could account for the increased toxicity observed. Direct analysis of such events, however, lies beyond the scope of the present study.

Do these observations have physiological relevance? Clearly, promoting the successful import of a protein is advantageous to the producing plant, especially in a dedicated storage tissue. Likewise, glycosylation has been associated with long term protein stability *in planta* (37). While the ribosomes of *R. communis* are sensitive to RTA (5), the ricin precursor is not enzymatically active (10). On the other hand, inefficient import, as we have seen when the propeptide is absent, would potentially lead to proteolytic processing of proricin and folding of the RTA moiety on the cytosolic surface of the ER membrane to generate a stable population of toxin capable of damaging *Ricinus* ribosomes. It is plausible that the spacing provided by the propeptide acts in concert with the synthesis of ricin as an inactive precursor and the relative recalcitrance of *Ricinus* ribosomes to reduce the possible toxic effects of this toxin's expression in endosperm tissue. Similarly, the two lysine residues in the catalytic polypeptide have been implicated in reducing toxicity in the producing tissue, in this case by permitting polyubiquitination and thus promoting the proteasomal degradation of any dislocated toxin or toxin-containing fragment (36). It is interesting therefore that the N-proximal of these conserved lysines (Lys-4) is also inhibitory to nascent chain import in the absence of the propeptide. Interestingly, a lysine residue adjacent to the propeptide is a feature of other RIPs (Fig. 1*A*, *underlined*).

The biosynthesis and mechanism of action of protein toxins such as ricin is of considerable current interest (38), particularly where toxin subunits are expressed in the secretory pathway both in plants and heterologous systems (9, 17, 20, 36, 39). The tissue that manufactures this potent toxin contains ribosomes that are themselves susceptible to its catalytic activity. The

question of how the plant protects itself during toxin synthesis is therefore of paramount importance and may have parallels to other systems in which sensitive cells express deadly poisons. Even within the plant kingdom, ricin (regarded as the archetypal RIP) is just one member of the 100+ RIP family (40). The mechanism of protection we describe may therefore be widespread in nature.

Together, our data suggest that the propeptide facilitates both the import and glycosylation of nascent preproricin and, in so doing, possibly helps to reduce the risk of exposing endogenous ribosomes to the deleterious effects of this potent toxin. Other ER-directed ribosome-inactivating proteins also seem to possess N-terminal propeptides (Fig. 1*A*). The precise sites of signal peptide cleavage in many other plant toxins are yet to be determined, and thus there are likely to be many more RIPs containing this spacer.

REFERENCES

1. Endo, Y., and Tsurugi, K. (1987) *J. Biol. Chem.* **262,** 8128–8130
2. Lord, J. M., Hartley, M. R., and Roberts, L. M. (1991) *Semin. Cell Biol.* **2,** 15–22
3. Montanaro, L., Sperti, S., Mattioli, A., Testoni, G., and Stirpe, F. (1975) *Biochem. J.* **146,** 127–131
4. Osborn, R. W., and Hartley, M. R. (1990) *Eur. J. Biochem.* **193,** 401–407
5. Hartley, M. R., Chaddock, J. A., and Bonness, M. S. (1996) *Trends Plant Sci.* **1,** 254–260
6. Lord, J. M. (1985) *Eur. J. Biochem.* **146,** 403–409
7. Lord, J. M. (1985) *Eur. J. Biochem.* **146,** 411–416
8. Roberts, L. M., and Lord, J. M. (1981) *Eur. J. Biochem.* **119,** 31–41
9. Ferrini, J. B., Martin, M., Taupiac, M. P., and Beaumelle, B. (1995) *Eur. J. Biochem.* **233,** 772–777
10. Richardson, P. T., Westby, M., Roberts, L. M., Gould, J. H., Colman, A., and Lord, J. M. (1989) *FEBS Lett.* **255,** 15–20
11. Harley, S. M., and Lord, J. M. (1985) *Plant Sci.* **41,** 111–116
12. Hara-Nishimura, I. (1995) *Seikagaku* **67,** 372–377
13. Hara-Nishimura, I., Inoue, K., and Nishimura, M. (1991) *FEBS Lett.* **294,** 89–93
14. Yamada, K., Shimada, T., Kondo, M., Nishimura, M., and Hara-Nishimura, I. (1999) *J. Biol. Chem.* **274,** 2563–2570
15. Tulley, R. E., and Beevers, H. (1976) *Plant Physiol.* **58,** 710–716
16. Yuole, R. J., and Huang, A. H. C. (1976) *Plant Physiol.* **58,** 703–709
17. Sehnke, P. C., Pedrosa, L., Paul, A.-L., Frankel, A. E., and Ferl, R. J. (1994) *J. Biol. Chem.* **269,** 22473–22476
18. Tagge, E. P., Chandler, J., Harris, B., Czako, M., Marton, L., Willingham, M. C., Burbage, C., Afrin, L., and Frankel, A. E. (1996) *Protein Expression Purif.* **8,** 109–118
19. Frigerio, L., Vitale, A., Lord, J. M., Ceriotti, A., and Roberts, L. M. (1998) *J. Biol. Chem.* **273,** 14194–14199
20. Di Cola, A., Frigerio, L., Lord, J. M., Ceriotti, A., and Roberts, L. M. (2001) *Proc. Natl. Acad. Sci. U. S. A.* **98,** 14726–14731
21. Frigerio, L., Jolliffe, N. A., Di Cola, A., Felipe, D. H., Paris, N., Neuhaus, J. M., Lord, J. M., Ceriotti, A., and Roberts, L. M. (2001) *Plant Physiol.* **126,** 167–175
22. Tabe, L., and Higgins, T. J. V. (1998) *Trends Plant Sci.* **3,** 282–286
23. Pedrazzini, E., Giovinazzo, G., Bielli, A., de Virgilio, M., Frigerio, L., Pesca, M., Faoro, F., Bollini, R., Ceriotti, A., and Vitale, A. (1997) *Plant Cell* **9,** 1869–1880
24. Chaddock, J. A., and Roberts, L. M. (1993) *Protein Eng.* **6,** 425–431
25. Day, P. J., Ernst, S. R., Frankel, A. E., Monzingo, A. F., Pascal, J. M., Molina-Svinth, M. C., and Robertus, J. D. (1996) *Biochemistry* **35,** 11098–11103
26. Bendtsen, J. D., Nielsen, H., von Heijne, G., and Brunak, S. (2004) *J. Mol. Biol.* **340,** 783–795
27. Wales, R., Richardson, P. T., Roberts, L. M., Woodland, H. R., and Lord, J. M. (1991) *J. Biol. Chem.* **266,** 19172–19179
28. Daubenfeld, T., Hossann, M., Trommer, W. E., and Niedner-Schatteburg, G. (2005) *Biochem. Biophys. Res. Commun.* **333,** 984–989
29. Taylor, S., Massiah, A., Lomonossoff, G., Roberts, L. M., Lord, J. M., and Hartley, M. (1994) *Plant J.* **5,** 827–835
30. Higy, M., Junne, T., and Spiess, M. (2004) *Biochemistry* **43,** 12716–12722
31. Gietl, C., and Schmid, M. (2001) *Naturwissenschaften* **88,** 49–58
32. Schmid, M., Simpson, D. J., Sarioglu, H., Lottspeich, F., and Gietl, C. (2001) *Proc. Natl. Acad. Sci. U. S. A.* **98,** 5353–5358
33. Nilsson, I. M., and von Heijne, G. (1993) *J. Biol. Chem.* **268,** 5798–5801
34. Rutkowski, D. T., Ott, C. M., Polansky, J. R., and Lingappa, V. R. (2003) *J. Biol. Chem.* **278,** 30365–30372
35. Goder, V., and Spiess, M. (2003) *EMBO J.* **22,** 3645–3653
36. Di Cola, A., Frigerio, L., Lord, J. M., Roberts, L. M., and Ceriotti, A. (2005) *Plant Physiol.* **137,** 287–296
37. Bustos, M. M., Kalkan, F. A., VandenBosh, K. A., and Hall, T. C. (1991) *Plant Mol. Biol.* **16,** 381–395
38. Bismuth, C., Borron, S. W., Baud, F. J., and Barriot, P. (2004) *Toxicol. Lett.* **149,** 11–18
39. Slominska-Wojewodzka, M., Gregers, T. F., Walchli, S., and Sandvig, K. (2006) *Mol. Biol. Cell* **17,** 1664–1675
40. Stirpe, F. (2004) *Toxicon* **44,** 371–383

The N-terminal Ricin Propeptide Influences the Fate of Ricin A-chain in Tobacco Protoplasts

Nicholas A. Jolliffe, Alessandra Di Cola, Catherine J. Marsden, J. Michael Lord, Aldo Ceriotti, Lorenzo Frigerio and Lynne M. Roberts

J. Biol. Chem. 2006, 281:23377-23385.
doi: 10.1074/jbc.M602678200 originally published online June 14, 2006
